Formation of an information network in a self-pulsating multimode laser

Kenju Otsuka,* Yoshihiko Miyasaka, and Tamaki Kubota
Department of Human and Information Science, Tokai University, 1117 Kitakaname, Hiratsuka, Kanagawa 259-1292, Japan

Jing-Yuan Ko
Department of Physics, National Kaohsiung Normal University, Ho-Ping First Road, Kaohsiung 802, Taiwan
(Received 29 September 2003; published 15 April 2004)

We investigated self-induced pulsations in a globally-coupled microchip multimode solid-state laser operating on a Λ transition. A variety of dynamic states, featuring locking of pulsation frequencies, multidimensional quasiperiodic, and chaotic pulsations, induced by nonlinear modal interactions were observed depending on the number of oscillating modes. The underlying modal interplay was characterized in terms of the dynamic statistical quantity of information circulations. Mode grouping and information sender-receiver-mediator relationships established among mode groups, i.e., "information networks," were identified. Observed dynamic states were reproduced by numerical simulation of a model equation and each dynamic state was shown to create its own information network.

DOI: 10.1103/PhysRevE.69.046201 PACS number(s): 42.55.Rz, 42.55.Xi, 42.65.Ky, 42.65.Sf

Over the past decade, much effort has gone into characterizing the complex behaviors in nonlinear systems. However, most of the methods used are applicable only to low-dimensional systems [1]. For high-dimensional systems, two promising methods based on information theory have been proposed. In one, the turbulence in high-dimensional systems is characterized using models of fluid turbulence and optical turbulence [2,3]. The turbulence is described in terms of dynamic connectivity in the wave-number space using the information-theoretic quantities of mutual information and the cross-information flow rates (CIFR), in which CIFR implies the rate of common information generated in the two time sequences per unit time which does not depend on the time lag between the two processes [2,3]. The second method was proposed by Palus *et al.* They introduced the conditional self-mutual information and "coarse-grained" transinformation rates (CTIR) [4,5]. CTIR implies the "average" rate of the net amount of information transferred from one time sequence to another, in which the averaging is carried out over the time at which the self-mutual information shows the first local minimum for all the data sets. In the second method, one can perform dynamic characterization of complex behaviors by calculating time-dependent CTIR from experimental temporal evolutions of coupled elements. Using this second method, they identified the causal drive-response relationship between two coupled chaotic systems from experimental bivariate time series and demonstrated the effectiveness of their method for characterizing synchronization phenomena in many physical and biological systems, especially in the fields of physiology and neurophysiology [5].

On the other hand, globally coupled multimode lasers are known to exhibit complex behaviors featuring antiphase dynamics. Therefore, among the many nonlinear systems, chaotic multimode lasers are a promising approach to information-theoretic characterization of the dynamic interplay among modes. Information circulation analysis based on CTIR [5] was applied to a two-mode or three-mode laser and causal relationships were identified among modes [6,7]. Meanwhile, a *modulated* three-mode laser [7] is the simplest example of globally coupled chaotic lasers. More rich dynamic behaviors, which go beyond three-mode lasers, and complicated information flows among modes are expected when the number of modes increases. Two intriguing questions then arise: What is the form of the interaction and resultant complex dynamics when the number of modes increases, and how can the dynamic interplay among modes be characterized in terms of information-theoretic approach? Motivated by these questions, we investigated the nonlinear dynamics of the model of a more general *self-pulsating* multimode laser and used information circulation analysis to identify the causal relationships established among the many coupled modes.

Multimode lasers operating on a Λ-scheme transition are promising candidates for experimentally investigating the nonlinear dynamics of the model of a self-pulsating multimode laser, in which pulsations arises through the nonlinear stimulated absorption due to the quantum interference of lower level atoms [8]. The purpose of the present paper is twofold: to demonstrate self-pulsations in a free-running multimode laser, without a doubling crystal, operating on multiple-Λ-schemes, and to characterize complex behaviors in terms of information-theoretic approach.

In the work described here, we used a free-running LNP laser, operating on the $^4F_{3/2}(1) \rightarrow {}^4I_{11/2}(1,2,3)$ transitions around the 1100-nm wavelength. In this system, multilongitudinal modes can oscillate on the different transitions forming the multiple-Λ schemes *without a doubling crystal*, because reabsorption effect is enhanced due to higher Nd densities in the lower manifolds, $^4I_{11/2}$, compared with those in the manifolds, $^4I_{13/2}$, based on the Boltzmann distribution. We demonstrated self-induced pulsations featuring locking of modal pulsation frequencies, multidimensional quasiperiodic pulsations, and the formation of an intermode informa-

*Electronic address: ootsuka@keyaki.cc.tokai-u.ac.jp

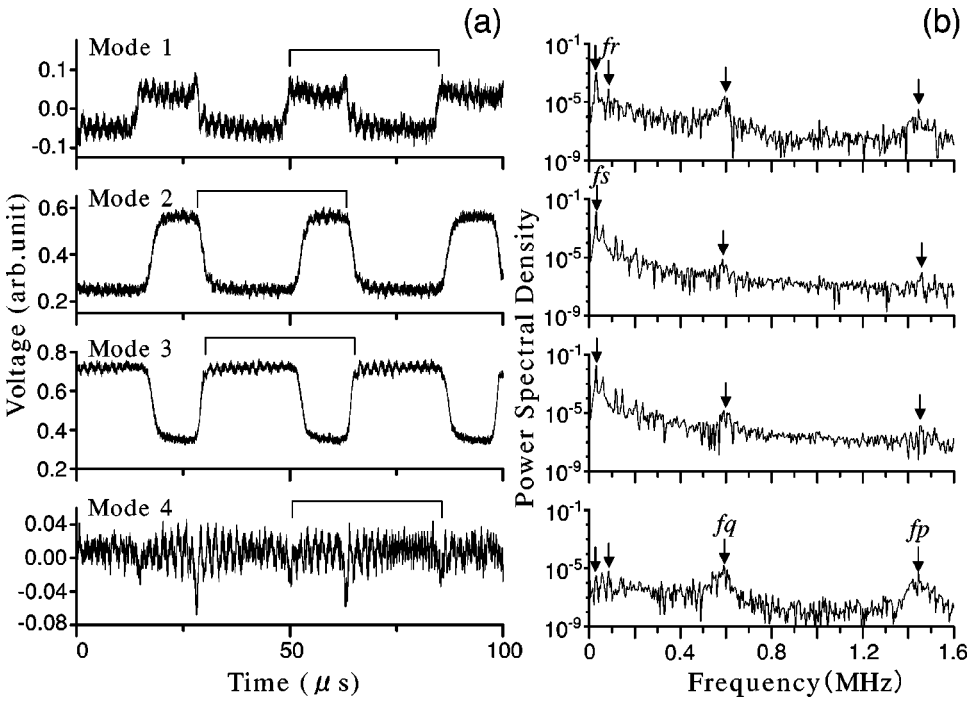

FIG. 1. Self-induced pulsations in the $[3,1,0]$ optical spectrum configuration with pump power $P=225$ mW and the threshold pump power $P_{th}=50$ mW. (a) Modal output wave forms and (b) corresponding power spectra. Modal intensities were measured simultaneously, but relative intensities were not calibrated. The lasing wavelength relation of individual modes **1**,**2**,**3**, and **4** are $\lambda_1<\lambda_2<\lambda_3<\lambda_4$.

tion network in high pump power regimes, featuring mode grouping and information sender-receiver-mediator relationships established among mode groups, which can never be observed in two-mode or three-mode lasers [6,7].

We will first explain the laser system we used. A model laser system for investigating multimode dynamics on a Λ transition was configured by controlling the operating condition of a laser diode (LD)-pumped 1-mm-thick LNP laser with directly coated mirrors M_1 (reflectivity $R_1>99.9$ % at lasing wavelengths; transmission >95 % at 808 nm) and M_2 ($R_2=98$ %). In LD-pumped stoichiometric LNP lasers with high Nd concentrations, simultaneous multitransition oscillations (MTOs) on ${}^4F_{3/2}(1)\rightarrow{}^4I_{11/2}(1,2,3)$ transitions with different emission cross sections are possible at wavelengths of 1048, 1055, and 1060 nm. These transitions form a Λ scheme, resulting from the significant transition-dependent reabsorption loss compared to the common cavity loss for different transitions [9,10]. The resulting effective net gains for different transitions can be controlled by changing the cavity (i.e., crystal) length and the common cavity loss [9,10]. Furthermore, the pump-density-dependent Auger recombination process inherent in stoichiometric lasers results in the smoothing of the spatial hole-burning effect [10]. In LNP lasers with a 100 μm absorption length for LD pumped light at a wavelength of 808 nm, the thermal lens effect (i.e., cavity diffraction loss) and the pump power density are easily controlled by changing the magnification of the microscope's objective lens to focus the pump beam on the LNP crystal or by defocusing the pump beam [11]. By changing the pump beam spot size, the cavity loss and the Auger recombination can be changed to control the MTO optical spectra and the number of adjacent longitudinal modes, separated by $\Delta\lambda$ ($=\lambda^2/2nL=0.34$ nm; λ—wavelength, n—LNP's refractive index, L—crystal length), on the different transitions [11]. In this way, various MTO optical spectra with different numbers of adjacent longitudinal modes on different transitions can be achieved. In the low pump regime below a Hopf bifurcation, the nonlinear stimulated absorption is less effective and stable MTOs occur [9,10]. In the high pump regime, on the other hand, self-induced pulsations appear via a Hopf bifurcation through the enhanced nonlinear stimulated absorption [8,12].

In such multimode operations on the Λ transition, complex dynamic instabilities resulting from the interaction of modes on different transitions should occur due to the enhanced nonlinear stimulated absorptions [8,12]. Example modal output wave forms and the corresponding power spectra are shown in Fig. 1 for $[1048,1055,1060]=[3,1,0]$ lasing optical spectra, i.e., three adjacent longitudinal modes **1**, **2**, and **3** on the 1048-nm transition and single longitudinal mode **4** on the 1055-nm transition. Each modal output beam passed through a monochrometer, and the signal detected using an InGaAs photoreceiver was delivered to a digital oscilloscope. For modes **1** and **4**, the ac output wave forms are displayed because the pulsation amplitudes were small compared to the average values. The modal pulsations in Fig. 1 have N relaxation oscillation frequencies (N—number of modes), as indicated by the arrows. Lower relaxation oscillation components except the highest frequency component are known to appear through cross-saturation dynamics of population inversions [9]. The f_s corresponds to the repetition frequency of square waves in modes **1**, **2**, and **3**, the f_r corresponds to an inverse of the square-wave width of mode

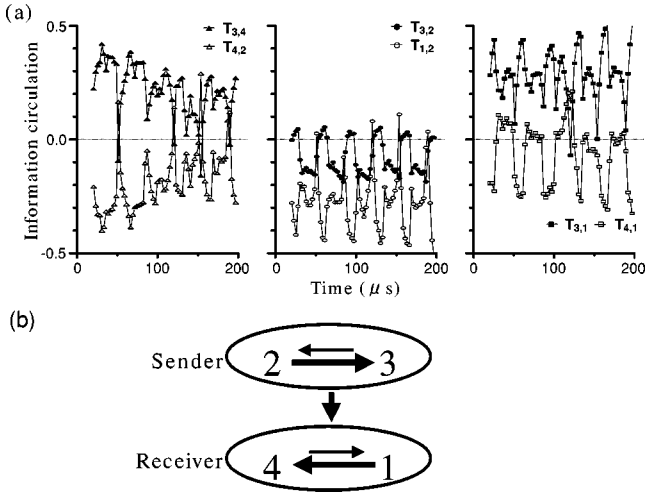

FIG. 2. (a) Information circulations and (b) information network corresponding to modal output wave forms in Fig. 1. Calculations were carried out using a moving window with a length of T_w =2048 data points (40.96 μs) and a moving step T_s with a length of 256 data points (5.12 μs), where the light intensity was partitioned into I_s=16 values to calculate intensity probability distributions. Ranges of time lag in the summation $\tau^*(i)$ were 62, 64, 54, and 24 data points with a delay step of T_d=40 ns for modes i=1,2,3,4, respectively.

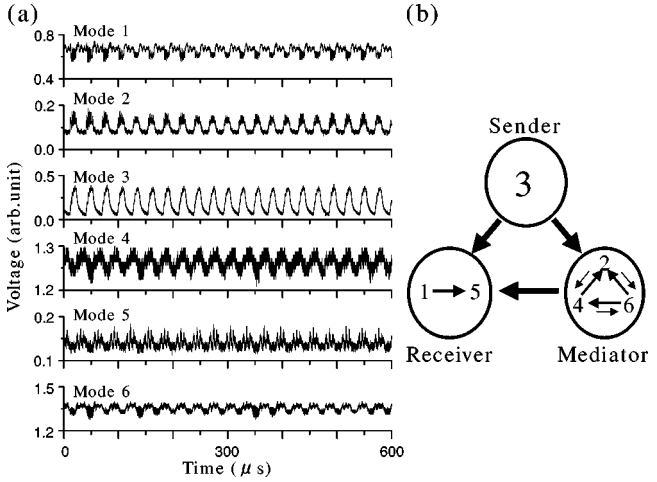

FIG. 3. Pulsations in [0,3,3] optical spectrum configuration with P=278 mW: (a) modal output wave forms and (b) information network. $\lambda_1<\lambda_2<\lambda_3<\lambda_4<\lambda_5<\lambda_6$. Information circulations were calculated assuming T_w=163.84 μs, T_s=20.48 μs, and $\tau^*(i)$=45, 49, 48, 18, 43, 11 data points for modes i=1,2,…,6, respectively, with a delay time step of T_d=40 ns and I_s=16.

2, which equals $3f_s$, and the f_q and f_p correspond to the frequencies of the faster oscillations seen in mode **4** and superimposed on square waves, particularly in mode **1**. It is interesting to note that frequency locking of $[f_p:f_q:f_r:f_s]$ =[50:20:3:1] occurs when f_s=30 kHz, at which point different pulsation wave forms are embedded for different modes in the common time interval indicated by the bridges ⊓, and they repeat periodically. It should also be noted that small-amplitude sinusoidal oscillations appeared just above the Hopf bifurcation point for modes **2** and **3** on the 1048 -nm transition, and "sine waves" quickly became "square waves" as the pump power was increased, suggesting a singular Hopf bifurcation [13].

Next, using the information-theoretic approach, we characterized the modal interplays occurring in complex pulsations. We used the information circulation analysis of long-term experimental time series [5,6] to identify causal relationships among globally coupled modes that arose due to the cross saturation of population inversions through spatial hole burning.

The information circulation is defined as: $T_{X,Y}=T_{X\to Y}-T_{Y\to X}$, $T_{X\to Y}=(1/\tau^*)\Sigma_\tau S(Y,Y_\tau|X)-(1/\tau^*)\Sigma_\tau S(Y,Y_\tau)$ is the information transfer rate from time series $X=\{x(t)\}$ to time series $Y=\{y(t)\}$, and $S(Y,Y_\tau)$ is the self-mutual information for Y. $S(Y,Y_\tau|X)$ is the conditional self-mutual information of time series X given time series Y; τ^* is the first local minimum of $S(Y,Y_\tau)$ [5,6].

The information circulations we calculated using the modal output time series in Fig. 1 are shown in Fig. 2(a). Information circulation $T_{i,j}$ is the "net" information flow among the two modes, and if $T_{i,j}>0(<0)$ the information flows from mode $i(j)$ to mode $j(i)$ [5,6]. In this case, the antiphased *periodic* square-wave modes **2** and **3** act as information senders, transferring the information to other receiver modes **1** and **4**. The information circulations also indicate that sender modes and receiver modes form each group, in which periodic reversal of the information flow direction at the square-wave frequency occurs among the modes in each group. The "information network" formed in the present scheme is depicted in Fig. 2(b), where the arrows indicate the directions of the net information flows.

When the pump power was increased, the 1048-nm mode intensity decreased and finally two transition oscillations, at 1055 and 1060 nm, became dominant due to the resonant reabsorption effect [9,10]. The modal pulsation wave forms observed in the [0,3,3] optical spectrum configuration, i.e., three adjacent longitudinal modes **1**, **2**, and **3** on the 1055-nm transition and modes **4**, **5**, and **6** on the 1060-nm transition are shown in Fig. 3(a). In this case, the locking of the pulsation frequencies failed, and multidimensional quasiperiodic motions appeared. Mode grouping occurred in the hierarchical information network formed in this case, as illustrated in Fig. 3(b). Similar to the [3,1,0] case shown in Fig. 2, *periodic* pulsating mode **3** acted as an information sender. The **1** and **5** modes, in one group, exhibited low-frequency envelope modulations (i.e., multidimensional quasiperiodic motions) and acted as information receivers, while the **2**, **4**, and **6** modes, in another group, exhibited more irregular motions and acted as information mediators. Here, an information mediator is defined as the mode which receives information from the sender and transfers it to the receiver. Simultaneous measurements of the modal output intensities showed that the low-frequency modulations were not due to noise and that the modal outputs were grouped into periodic and quasiperiodic motions. A sender-receiver relationship was established within grouped modes (**1** and **5**), and periodic reversal of the information flow directions occurred within grouped modes (**2**, **4**, and **6**). Each mode in the information mediator group, which exhibited rather irregular

motion, received each information from the *periodic* sender mode **3** and transferred it both to the "quasiperiodic" receiver modes **1** and **5**. When the pump density was increased by focusing the pump beam tightly on the LNP laser, the number of adjacent longitudinal modes were decreased through the enhanced Auger recombination effect [10,11]; as a result, the $[0,1,1]$ configuration was attained. In this case, simple antiphase pulsations were observed; the information flow occurred from the 1055-nm mode to the 1060-nm mode.

Finally, we show an example of numerical result that shows such essential features in observed behaviors as locking, mode grouping, and hierarchical information network formation between globally coupled modes. The model equations given below were enhanced by adding nonlinear stimulated absorption terms [12] to the MTO laser rate equations in order to include cross saturation and resonant absorption more explicitly [9].

$$\frac{dn_k}{dt} = w - n_k - g_k n_k (s_k + \sum \beta_{k,j} s_j), \tag{1}$$

$$\frac{ds_k}{dt} = K\left\{\left[g_k n_k - \Gamma_k - g_k \sum \frac{R_{k,j}}{K}(n_k + n_j)s_j\right]s_k + \epsilon n_k\right\}, \tag{2}$$

$$k = 1,2,3,4, j \neq k.$$

Here, w is the relative pump power normalized by the first-mode threshold, n_k is the normalized population inversion density of the kth mode, s_k is the normalized photon density, K is the fluorescence-to-photon lifetime ratio τ/τ_p, time is scaled by the fluorescence lifetime, g_k is the modal gain ratio with respect to the first mode, $\Gamma_k (=[L_0 + 2\alpha_k L]/[L_0 + 2\alpha_1 L])$ is the modal loss ratio (L_0—common cavity loss, α_k—reabsorption coefficient), $\beta_{k,j}$ is the cross-saturation coefficient, and ϵ is the spontaneous emission rate. Additionally, $R_{k,j}$ is the nonlinear stimulated absorption coefficient resulting from quantum interference among lower level atoms and is represented by the lower-level-to-photon lifetime ratio, τ_L/τ_p [12].

In numerical simulation, we assumed the spectroscopic data of the LNP laser for three transitions [9] and the $[2,1,1]$ lasing optical spectrum, in which two adjacent longitudinal modes (**1** and **2**) on the 1048-nm transition and single modes **3** and **4** on the 1055- and 1060-nm transitions, respectively, i.e., $R_{1,2}=0$. The Hopf bifurcation occurred at $w=3.35$ in the three-mode regime, below the threshold of the 1060-nm mode ($w=3.65$).

The bifurcation diagram in four-mode regimes is shown as a function of the relative pump power in Fig. 4, in which the locking ratio $[f_p:f_q:f_r:f_s]$ and the largest Lyapunov exponent are indicated. Modes **1** and **2** on the 1048-nm transition exhibited the same periodicity, and chaotic regions appeared between different locking states, indicating an abrupt increase in the largest Lyapunov exponent. Example simulated wave forms exhibiting $[f_p:f_q:f_r:f_s]=[15:15:5:3]$ locking in Fig. 4 are shown in Fig. 5(a). The simulated hierarchical information network is shown in Fig. 5(b). Modes

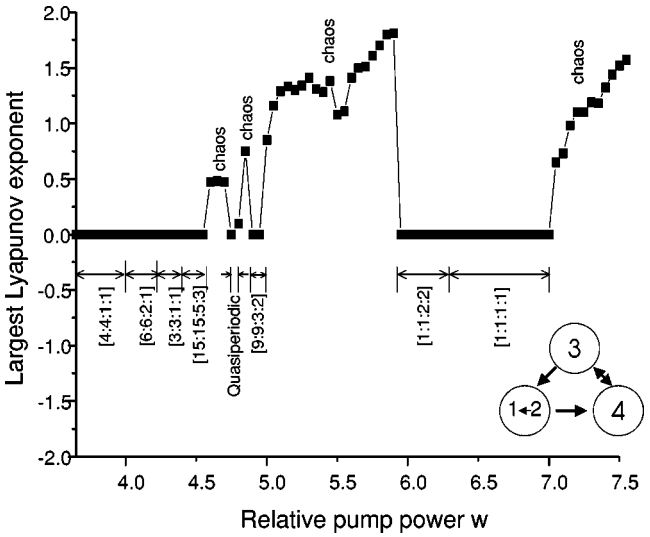

FIG. 4. Bifurcation diagram and largest Lyapunov exponent as a function of relative pump power for $K=1000$, $L_0=0.07$, and $L=1$ mm. Other values relevant to the LNP laser are [9] $\beta_{1,2}=0.923$, $\beta_{j,k}(j\neq 1, k\neq 2)=2/3$, $g_1=1$, $g_2=0.95$, $g_3=0.50$, $g_4=0.41$, $\alpha_1=\alpha_2=0.11$ cm^{-1}, $\alpha_3=0.0407$ cm^{-1}, $\alpha_4=0.0253$ cm^{-1}, $R_{j,k}(j\neq 1, k\neq 2)=2$, and $\varepsilon=1.2\times 10^{-7}$. The information circulation for $[1:1:1:1]$ locking is depicted in the inset.

are divided into groups, and each group plays a different role, as in Fig. 3. Mode **2** acts as the information sender, mode **4** acts as the receiver, and grouped mediator modes **1** and **3** receive the information from sender mode **2** and transfer it to receiver mode **4**. It is interesting to note that although modes **1** and **2** show similar wave forms, they play different roles in the information network. Another interesting point is that balanced bidirectional information flows,

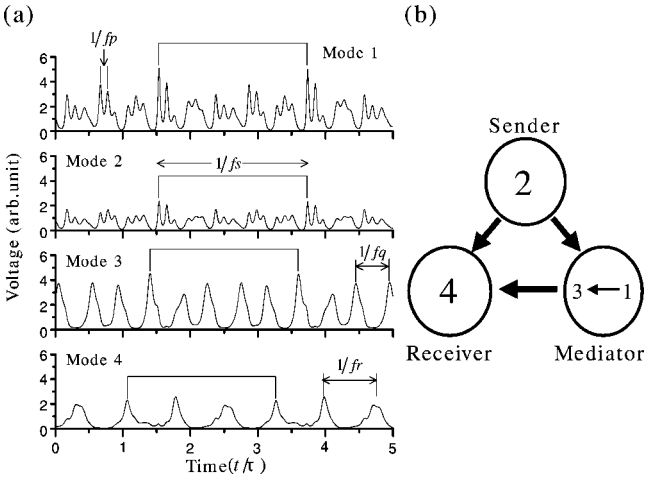

FIG. 5. (a) Example simulated wave forms in region of $[15:15:5:3]$ locking (shown in Fig. 4) with $w=4.5$. Other parameters are the same as in Fig. 4. (b) Information network obtained from numerical time series of Fig. 5(a). The information circulation was calculated assuming $T_w=4096$ data points (time step: 10^{-3}), $T_s=512$ data points, and $\tau^*(i)=40$, 41, 71, 107 data points for modes $i=1,2,3,4$, respectively, with a delay time step of $T_d=10^{-3}$ and $I_s=16$.

TABLE I. Information networks created in different dynamic states shown in Fig. 4. S, M, R denote information sender, mediator and receiver, respectively.

States	Mode 1	Mode 2	Mode 3	Mode 4
4:4:1:1	R	R	S	M
6:6:2:1	M	R	M	S
3:3:1:1	M	R	S	M
15:15:5:3	M	S	M	R
Chaos	M	S	R	M
Quasiperiodic	R	S	M	M
Chaos	R	S	M	S
9:9:3:2	R	S	M	R
Chaos	S	M	M	R
1:1:2:2	M	M	S	R
1:1:1:1	M	M	S/M	R/M
Chaos	M	M	S	R

i.e., net information flow $T_{3,4}=0$, occur between modes **3** and **4**, which exhibit different periodic pulsations. It should be noted that each dynamic state in Fig. 4 including chaotic states was found to form its own information network, featuring grouping and sender-mediator-receiver relationship. Results are summarized in Table I. As for $[1:1:1:1]$ locking in the high pump region, balanced bidirectional flows between modes **3** and **4** appeared as shown in the inset of Fig. 4. The dynamical independence [14] in terms of information transfer rates summarized in Table I may have reflected to the system symmetry, i.e., modal intensity ratios, because relaxation oscillation frequencies depend on modal intensities [15]. Furthermore, it is interesting to note that mode **2** is considered to act as a leading mode for creating information networks because it plays the same role for a finite pump-power region and changes its role successively as receiver $\rightarrow$ sender $\rightarrow$ mediator, as the relative pump-power increases.

The essential features of observed dynamic states and information networks have been reproduced qualitatively in the present simulation. However, the quantitative reproduction of experimental results in a wide parameter region is necessary for understanding the meaning of the information circulation and its link with the underlying physics.

In summary, we investigated complicated self-pulsations in a free-running multimode laser operating on multiple-Λ-schemes. Locking of pulsation frequencies and multidimensional quasiperiodic motions were observed. Modal interplay behind the observed pulsations was characterized by information circulation analysis of the experimental time series and of the self-induced formation of information networks, in which each dynamic state forms its own information network. Mode grouping and information sender-mediator-receiver relationships among groups were identified. Observed dynamic states and the formation of information networks were reproduced by simulation of the model equations. Information circulation analysis could thus be a useful way for characterizing the dynamic interplay among many coupled elements in general complex systems with large coupled degrees of freedom in terms of information theory, i.e., information transfers between elements. The meaning of the information flow and its link with the underlying physics would be the intriguing subject to be studied.

[1] See, for example, *Dimensions and Entropies in Chaotic Systems*, edited by G. Mayer-Kress (Springer-Verlag, Berlin, 1986).

[2] K. Ikeda and K. Matsumoto, Phys. Rev. Lett. **62**, 2265 (1989).

[3] K. Ikeda, K. Otsuka, and K. Matsumoto, Prog. Theor. Phys. Suppl. **99**, 295 (1989).

[4] M. Palus, Physica D **93**, 64 (1996).

[5] M. Palus, V. Komarek, Z. Hrncir, and K. Sterbova, Phys. Rev. E **63**, 046211 (2001).

[6] K. Otsuka, J.-Y. Ko, T. Ohtomo, and K. Ohki, Phys. Rev. E **64**, 056239 (2001).

[7] K. Otsuka, T. Ohtomo, A. Yoshioka, and J.-Y. Ko, Chaos **12**, 678 (2002).

[8] K. Otsuka, E. A. Viktorov, and P. Mandel, Europhys. Lett. **45**, 307 (1999).

[9] R. Kawai, Y. Asakawa, and K. Otsuka, IEEE J. Quantum Electron. **35**, 1542 (1999).

[10] K. Otsuka, P. Mandel, and E. A. Viktorov, Phys. Rev. A **56**, 3226 (1997).

[11] Y. Asakawa, R. Kawai, K. Ohki, and K. Otsuka, Jpn. J. Appl. Phys., Part 1 **38**, L515 (1999).

[12] G. Kozyreff and P. Mandel, Phys. Rev. A **61**, 033813 (2000).

[13] T. Erneux, *Laser Bifurcations* (Northwestern University, Evanston, 1990).

[14] A. G. Vladimirov, E. A. Viktorov, and P. Mandel, Phys. Rev. E **60**, 1616 (1999).

[15] P. Mandel, M. Georgiou, K. Otsuka, and D. Pieroux, Opt. Commun. **100**, 341 (1993).